HHS Public Access

Author manuscript

Nat Med. Author manuscript; available in PMC 2016 June 01.

Published in final edited form as:

Nat Med. 2015 June ; 21(6): 647–653. doi:10.1038/nm.3860.

Common clonal origin of central and resident memory T cells following skin immunization

Olivier Gaide[1], **Ryan O. Emerson**[2], **Xiaodong Jiang**[1], **Nicholas Gulati**[3], **Suzanne Nizza**[1], **Cindy Desmarais**[2], **Harlan Robins**[4], **James G. Krueger**[3], **Rachael A. Clark**[1], and **Thomas S. Kupper**[1]

[1]Department of Dermatology, Brigham and Women's Hospital, Boston, MA

[2]Adaptive Biotech, Seattle, WA

[3]Laboratory for Investigative Dermatology, The Rockefeller University, New York, NY

[4]Fred Hutchinson Cancer Research Center, Seattle, WA

Abstract

Central memory T (T_{CM}) cells in lymph nodes (LN) and resident memory T (T_{RM}) cells in peripheral tissues play distinct roles in protective immunity[1-5]. Both are generated after primary infections, but the clonal origin of T_{RM} and T_{CM} cells is unclear. To address this question, mice were immunized through the skin with either a protein antigen, a chemical hapten, or a non-replicating poxvirus. We then analyzed antigen activated T cells from different tissues using high-throughput sequencing (HTS) of the gene *(Tcrbv)* encoding T cell receptor gene β chain CDR3 region to simultaneously track thousands of unique T cells[6]. For every abundant T_{RM} clone generated in the skin, an abundant T_{CM} clone bearing the identical TCR was present in lymph nodes (LN). Thus antigen reactive skin T_{RM} and LN T_{CM} clones were derived from a common naive T cell precursor after skin immunization, generating overlapping TCR repertoires. Although they bore the same TCR, T_{RM} mediated rapid contact hypersensitivity (CHS)[7] responses in mice, whereas T_{CM} mediated delayed and attenuated responses. Studies in human subjects confirmed the generation of skin T_{RM} in allergic contact dermatitis. Thus, immunization through skin simultaneously generates skin T_{RM} and LN T_{CM} in similar numbers from the same naïve T cells.

T_{RM} are known to be important in protective immunity, but their origin and relationship to other memory T cell subsets remains obscure. We previously demonstrated that both T_{RM} and T_{CM} were generated after Vaccinia skin infection[8,9] but the lineage commitment of

---

Correspondence: Thomas S. Kupper, Harvard Skin Disease Research Center, Department of Dermatology, Brigham and Women's Hospital, 77 Av. Louis-Pasteur, Boston, MA 02115, USA, tkupper@partners.org.
OG: Current address:
Dr. Olivier Gaide, Department of Dermatology, CHUV, 29 Av. de Beaumont, 1011 Lausanne, Switzerland, olivier.gaide@chuv.ch

AUTHOR CONTRIBUTIONS. O.G. and T.S.K. conceived and planned the study, reviewed experiments, analyzed data, and wrote the paper. O.G., R.O.E., X.J., N.G., S.N. performed experiments. H.S.R., R.O.E., C.D. and J.G.K. helped plan experiments and analyze data, and R.A.C. helped analyze data and edit the paper.

COMPETING FINANCIAL INTERESTS

R.O.E. and C.D. have full-time employment and equity ownership at Adaptive Biotechnologies Corporation. H.S.R. has consultancy, patents and royalties, and equity ownership at Adaptive Biotechnologies Corporation.

The authors declare no competing financial interests.

individual naive T cells to T_{RM} or T_{CM} in vivo was not addressed. Studies of endogenous naive T cells in vivo have suggested a one cell, one fate paradigm [5,10-13]. One report demonstrated that differentiation of individual naive CD4 cells into effector (T_{eff}) or follicular helper T (T_{FH}) cells was determined by TCR affinity for antigen[13], while another report showed that microenvironmental factors influenced the differentiation of individual naive CD8 cells into T_{EM} or T_{CM}, respectively[12]. In contrast, other studies using naive TCR transgenic CD8 T cells demonstrated that commitment of single T cells to T_{EM} or T_{CM} lineage was stochastic[14,15], a finding inconsistent with the one cell, one fate paradigm. To explore the origin of T_{CM} and T_{RM} further, we used three different antigens to immunize mouse skin: ovalbumin (OVA) with adjuvant (cholera toxin, CT), a contact sensitizer (dinitrofluorobenzene, DNFB), and a poxvirus (Modified Vaccinia Ankara; MVA) (**Supplementary Fig. 1**). In OVA+CT experiments, OT-I transgenic T cells, bearing a TCR specific to $OVA_{257-264}$, were injected into mice pre-immunization as an internal control (**Supplementary Fig. 1**). After each immunization, acute inflammation had resolved completely by day 35, and resting CD4 and CD8 T cells remained at the antigen treated site (**Supplementary Fig. 2 and 3**, refs [8,16]). We extracted DNA from skin and LN of individual mice before and at different time points after immunization, and HTS of the *Tcrbv1* gene was performed as previously described[6,17,18]. After 35 days, expanded T cell clones that were undetectable prior to immunization were considered antigen-specific, and the most abundant memory T cell clones (detectable at ≥5 copies/400 ng DNA at the site of antigen encounter) were studied further. After OVA + CT application, T cellclones present in both immunized ear and in distant unchallenged skin are represented as blue dots, corresponding to unique CDR3 sequences (**Fig. 1a**), consistent with our previous finding that skin infection generates antigen-specific T_{RM} clones in both treated and distant skin[8]. The most abundant shared clones are enclosed within the blue box (including the transgenic OT-1 clone) (**Fig. 1a**). The anatomic distribution of six expanded T cell clones in skin and LN's are shown in Fig. 1b, and only the OT-1 CDR3 is present in inguinal LN pre-immunization. The data are expressed as “clone frequency”, while all clones are present in both skin and LN post-immunization, the value for each clone is lower in LN than in skin (**Fig. 1b**). Because the absolute number of T cells is much higher in LN than in skin, we measured the total number of T cells of a particular clone in skin versus LN by measuring the number of CDR3-identical T cells per 400 ng of genomic DNA. By this analysis, T_{RM} in skin and T_{CM} in LN with the same CDR3 sequences were present in comparable abundance after OVA + CT immunization (**Supplementary Fig. 1**). The overlap of unique clones in skin and LN, as well as the average clone size in each compartment, are shown in **Fig. 1c**. Comparable results were obtained after DNFB exposure (**Fig. 1d,e,f**) and MVA exposure (**Fig. 1g,h,i**). For all three types of immunization, T cells in treated and distant skin (T_{RM}) as well as draining and distant LN contained common expanded memory T cell clones that were not detectable before immunization. Memory T cells enter distant LN directly from blood through high endothelial venules rather than afferent lymphatics; thus, memory T cell clones in distant LN were considered T_{CM}. In all mice from all groups combined, 85-93% of T_{RM} cell clones that were expanded at both skin sites were mirrored by CDR3-identical LN T_{CM} in similar abundance (n=41; **Fig. 1j**). We concluded that these T_{RM} and T_{CM} were derived from common naïve T cell precursors.

We next studied T cell responses following multiple applications of the hapten DFNB to the same skin site (**Fig. 2a**). Tissue harvest and HTS were performed at day 90 (**Fig. 2b,c,d**). The abundance of T cells in particular VJ groups were compared between three skin sites-- the tail (no DNFB), the right ear (DNFB × 2) and the left ear (DNFB × 6)-- and in the LN draining these sites (**Fig. 2b**). The expansion of individual VJ groups as a function of DNFB exposure was greater in the skin than the LN. In terms of V13.3/J2.2 T cell clones, three dominant clones (clones 1, 2 and 3) were expanded in both skin and LN. These same three abundant V13.3/J2.2 clones were consistently present in skin and lymph node (**Fig. 2d**). To rule out possible peripheral blood contamination of our tissue samples, we examined blood T cells by HTS of the *Tcrvb1* gene at the same time point (**Supplementary Fig. 2**). We found that the nine out of the ten most abundant T cell clones in blood were undetectable in skin and LN (**Supplementary Fig. 2a**); conversely, the most abundant clones in skin and LN were either absent or rare in blood (**Supplementary Fig. 2a**). Thus, our results cannot be attributed to peripheral blood contamination. After 6 DNFB, the most abundant clones in skin were between 7-17 times more numerous in skin than in LN (**Fig. 2e,f**). We conclude that multiple exposures of the same antigen to skin lead to preferential expansion of skin T_{RM}. Increased numbers of both CD4 and CD8 T cells (**Supplementary Fig. 3**) expressing a T_{RM} phenotype were present in skin (**Supplementary Fig. 4**).

We next joined DNFB sensitized mice to naive mice by parabiotic surgery (**Fig. 3a**). After 4 weeks of parabiosis followed by separation for two weeks, multiple shared clones were identified in the LN of the naïve and immunized parabiont, confirming free transfer of T_{CM} between parabiotic mice (**Supplementary Fig. 5**). While a very small number of shared clones appeared to be shared in the skin after parabiosis and separation (**Supplementary Fig. 5**), this difference was not statistically significant (p=0.1). These data demonstrate by *Tcrvb1* gene sequencing that T_{CM} are freely migratory, and T_{RM} in skin are sedentary. Despite the rapid equilibration of T cells between LN's in our parabionts[8], there was low absolute concordance of T cells (% of total unique CDR3 sequences shared) between these lymph nodes (~3%). To explore this further, we performed additional experiments and determined that overlap of total unique CDR3 sequences between two different lymph nodes in the same normal 6 week old mouse was actually very low (roughly 1%, **Supplementary Fig. 6**). This number did not increase appreciably 4 weeks after DNFB sensitization. In the same mouse, overlap of unique CDR3 sequences between skin sites was 5% before, and 11% after, DNFB sensitization (**Supplementary Fig. 6**). However, when expressed as the overlap of total CDR3 sequences in skin (accounting for the abundance of certain clones), the values were 20% before, and 50% after DNFB sensitization, consistent with results shown in **Figure 2**. The overlap of total CDR3 sequences in LN rose from 5% to 7% after DNFB (**Supplementary Fig. 6**), emphasizing that while expanded memory T cell clones are detectable in LN, they are greatly outnumbered by naïve T cells. In contrast, skin contains only memory T cells.

Our data show that skin T_{RM} and LN T_{CM} generated by the same immunization share identical *Tcrbv1* CDR3 sequences. We used parabiotic mice[8] and DNFB sensitization (**Fig 3a**) to examine the relative contributions of T_{RM} and T_{CM} to skin contact hypersensitivity (CHS), a mouse model of human allergic contact dermatitis (ACD)[7,19,20] . Previously

sensitized parabiotic mice manifested robust ear swelling 24 hours after DNFB challenge (**Fig 3b**), consistent with the kinetics of a T_{RM} response. Unsensitized (naïve) parabiotic mice (that contain DNFB-specific T_{CM} but not skin T_{RM}) manifested no increased ear swelling at 24 hours, but developed a delayed response five days after challenge (**Fig 3b**). Pre-treatment of these unsensitized parabiotic mice with FTY-720, a sphingosine 1 phosphate receptor inhibitor (Supplementary Fig. 7), abrogated this delayed ear swelling response (**Fig 3c**), consistent with a requirement for T_{CM} migration from LN. In contrast, FTY-720 had no effect on the rapid ear swelling response to DNFB challenge seen in the sensitized parabiotic mice (**Fig 3c**), confirming that this response was independent of T cell recruitment or migration [9,21]. These data are consistent with the rapid kinetics and durability of the T_{RM} response to antigen, in contrast to T_{CM}, specific for the same antigen. Complementary results were obtained in adoptive transfer studies at these time points (**Supplementary Fig. 7, 8 and 9**).

When the unsensitized ear of the sensitized parabiotic mice was challenged with DNFB, swelling of rapid kinetics (24 hours), though lower in magnitude, was observed (**Fig. 3d**). This is consistent with skin antigen challenge leading to global seeding of skin with antigen specific T_{RM}. In contrast, naïve unsensitized parabiotic mice showed no rapid ear swelling (24 hours) in either ear (**Fig. 3d,h**). Delayed ear swelling in both ears of these mice was observed at day 5 (**Fig. 3d,h**), which was abrogated by pre-treatment with FTY-720, confirming that the delayed response was mediated by T_{CM} (**Fig. 3e**). However, four weeks later, when these same mice were subsequently re-challenged on sensitized ear, rapid swelling now occurred at 24 hours (**Fig. 3f,g**). This is consistent with *de novo* generation of T_{RM} in these mice.

We next asked if T_{RM} could be observed in the skin of human subjects with ACD. Healthy individuals (n=11, males and females, aged 29-58) were sensitized to the contact allergen diphenylcyclopropenone (DPCP) at day - 14 on arm skin, and then challenged with DPCP on left thigh skin at day 0, with placebo challenge to right thigh skin (**Fig. 4a**)[22]. Biopsies were taken of the challenged (or placebo/mock challenged) leg skin sites at day 3, and also of the challenged leg skin site at both day 14 and month four after challenge, and photographic and microscopic analysis was performed. Clinically and microscopically, DPCP-challenged skin was inflamed at 3 and 14 days, but this had resolved by 4 months (**Fig. 4b**). In three of these individuals (selected randomly), DNA was extracted from skin biopsies and HTS of the *TCRBV1* gene was performed. Clones in placebo challenged skin (presumably generated by sensitization) were compared with those of DPCP-challenged skin at day 3, and we identified a number of shared clones (**Fig 4c**, blue dots are unique CDR3 sequences). Five representative clones (1-5, red box, **Fig 4c**) were also identified in day 14 post challenge and month 4 post challenge skin (**Fig 4d).** The absolute number of each of these five T cell clones increased over time and remained high at 4 months (**Fig 4e**), closely following the pattern and kinetics of antigen specific T_{RM} clones from our mouse studies. Additional T cell clones observed were present in placebo treated skin, but these other clones either did not change or decreased over the course of the experiment (clones a-d, **Supplementary Fig. 10**), and others did not appear until 14 days after challenge (**Supplementary Fig. 10**), after which point their abundance decreased. These clones did

not fit the criteria of T_{RM}, and are consistent with a recent report showing that only a subset of T cells in human skin are authentic T_{RM}.[23]

In this study, we used HTS of the *Tcrvb1* gene to explore the generation, localization and function of T_{RM} and T_{CM} in response to three types of skin immunization: a contact sensitizer hapten, a protein, and a virus. This approach allowed comprehensive characterization of the endogenous αβ T cell repertoires in normal nontransgenic mice[24]. After all immunizations, we observed the generation of comparable numbers of both T_{RM} and T_{CM} clones, residing in distinct anatomic compartments, from unique naïve T cell precursors. Although one previous report showed that T_{RM} were derived from KLRG-1^{lo} precursors, the development of T_{RM} from individual naive T cells has, to our knowledge, not been directly studied before[25]. In our study, the tissue T_{RM} compartment provided rapid, tissue specific responses to antigenic challenge, while the T_{CM} compartment was slower to manifest effector function but could supplement the T_{RM} compartment after antigen challenge. While analysis of *Tcrvb1* CDR3 sequences by HTS can yield false negatives, false positives are generally not observed, suggesting that the 93% overlap at the level of common unique CDR3 sequences (**Fig. 1h**) may underestimate the true concordance between skin T_{RM} and LN T_{CM}. These data are consistent with a common naïve T cell precursor of T_{RM} and T_{CM}, and therefore do not support the model of differentiation being determined by variables like TCR affinity or signaling strength[5,10-13] Repetitive antigenic challenges to skin led to preferential expansion of skin T_{RM}. We further demonstrated that T_{RM} mediate CHS, the mouse counterpart of human ACD, an acquired human disease that has limited effective therapies and a high economic impact[7]. Our studies on ACD in human subjects using HTS of the TCRVB gene are supportive of our mouse data. That ACD is mediated by T_{RM} helps to explain the recalcitrant, recurrent, and site-specific nature of this disease, and opens up new opportunities for therapies. By extension, we believe that many human immunologic diseases that recur episodically in barrier tissues (e.g., psoriasis, inflammatory bowel disease) may be mediated by T_{RM}. In summary, our observations suggest that after skin immunization, the immune system distributes TCR-identical antigen reactive T cells both to LN (as T_{CM}) and to the peripheral tissues (as T_{RM}), thus generating two compartments of memory T cells with identical antigen specificity but different effector properties.

METHODS

Study subjects and skin samples

Skin biopsies of DPCP challenge reactions and placebo-treated sites were obtained from 11 volunteers under a protocol approved by The Rockefeller University's Institutional Review Board[22]. We obtained written informed consent from all subjects and the study adhered to the Declaration of Helsinki Principles. Consent to publish was obtained for all subjects who were photographed. The immunization with DPCP (Hapten Pharmaceuticals), the recall and the sampling have been described before[22]. Briefly, we sensitized healthy individuals to DPCP and 2 weeks later challenged them with two applications (0.04%) on their left thigh and two placebo applications on their right thigh (11 individuals, male and female aged 29-58). We took skin biopsies at day 3, 14 and month 4 post challenge, and stored them at

−80C until processed. For 3 subjects (1 female, 2 males, aged 46-55, selected randomly), HTS was performed on all biopsy samples.

Animal experiments

We purchased C57BL/6 mice (5-7 weeks of age, females) from The Jackson Laboratory, Bar Harbor, ME. Purchased mice had at least one week of acclimation in the animal facility of Harvard Institutes of Medicine, Harvard Medical School, before the initiation of any experiment. We bred and housed C57BL/6J *Thy1.1 Rag1*−/−Tg(TcraTcrb)1100Mjb/J (better known as OT-I) mice at the same facility. We performed all animal experiments in accordance with the guidelines set out by the Center for Animal Resources and Comparative Medicine at Harvard Medical School. For all experiments, animals were randomized in the different experimental groups by the animal facility staff, so that the investigator did not select groups based on size or appearance, but the investigator was not blinded once the experiments were initiated. Mice: groups of 3 for naive or simple DNFB positive mice were sufficient as ear swelling is highly reproducible (pooled naive of positive control in this paper = 36 mice). For other conditions, we chose groups of 5 mice as prior publications had identified it as the correct number (statistic power reached, minimal animal number). The sole exclusion criterion was death of the subject animal (1 occurrence of unknown cause, others due to complications linked with the surgical procedure).

Antigen challenge to skin

We sensitized C57BL/6 mice by topical applications of 20 μl of 0.25% DNFB diluted in acetone olive oil (3:1 v/v) at the indicated time points (day 0, 1, or 0, 1 and 7). Challenged was performed at the indicated time points with 20 μl of DNFB-acetone olive oil (aOO) (0.25%). We measured ear thickness with a digital thickness gauge (Mitsutoyo) before and after DNFB challenge. For OVA+CT immunization, mice were immunized epicutaneously as previously described[8]. Briefly, we used scotch tape (3M) to gently remove the cornified layer of ear skin, and then treated the skin with acetone and cholera toxin adjuvant (List Biological Labs) before administration of chicken Ovalbumin + Cholera toxin. For OT-I experiments, we transferred 1×10^4-$1x10^6$ OT-I splenocytes intravenously into recipient mice, and when applicable 24 h prior to LN dissection and biopsy. We performed epicutaneous infection by scarification as previously described[9]. A minimum of three, and typically five mice per group were used for all experiments, and every experiment was performed at least twice (and often multiple times). We used Fingolimod (FTY-720, Sigma) diluted in PBS and injected it intraperitoneally at 1 μg/g mouse; e.g., typically 25μg/mouse i.p. daily for 7 days, beginning 2 days before the DNFB challenge.

Parabiotic surgery

We performed parabiosis surgery as previously described[8]. Briefly, we shaved the flank of sex- and age-matched mice one day prior to surgery. We then anaesthetized them to full muscle relaxation with ketamine and xylazine (10mg/g) i.p. After skin disinfection (betadine solution and 70% ethanol three times), we made two matching skin incisions from the olecranon to the knee joint of each mouse pair. We then bound the elbow and knee joints by a single 5-0 silk suture, and closed the dorsal and ventral skins with staples and 5-0 silk

suture. Betadine solution was used to cover the full length of the dorsal and ventral incision. We kept the mice on heating pads and continuously monitored them until recovery from anesthesia and surgery. We used 2.5 mg/g flunixin s.c. for analgesia every 12h for 48h after the operation. After an interval of the indicated weeks, parabiotic mice were surgically separated by a reversal of the above procedure for subsequent experiments.

Lymphadenectomy

Briefly, we shaved mice were on the flank and belly one day prior to surgery. We anaesthetized the mice one day later to full muscle relaxation with ketamine and xylazine (10mg/g) i.p. After skin disinfection (betadine solution and 70% ethanol three times), we performed a 1 cm skin incision on a longitudinal line 0.5 cm medial to the mammary gland. We everted the lateral skin to reveal the inguinal lymph node, which we then excised. We closed the incision with 2 surgical clips, disinfected with betadine 1% and kept the mice were kept on heating pads and continuously monitored until recovery. We used 2.5 mg/g flunixin s.c. for analgesia every 12h for 24h.

Viruses and infections

We obtained recombinant MVA from B. Moss (NIH) and grew them on DF-1 cells. Viral titers were determined using CV-1 cells and 2×10^6 p.f.u. of MVA used for epicutaneous infection by skin scarification, as previously described[8].

Preparation of cell suspensions

We harvested lymph nodes and spleen and passed them through a 70-mm nylon cell strainer to prepare cell suspensions, in which we lysed red blood cells with hypotonic solution (Gibco). For skin tissue, we removed hair, chopped skin into small fragments and incubated them in Hanks balanced salt solution (Gibco) supplemented with 1 mg/ml collagenase A (Pharmingen) and 40 mg/ml DNase I (Roche) at 37C for 30 min. After filtering through a 70-mm nylon cell strainer, we collected the cells and washed them thoroughly with cold PBS before staining.

Antibodies and flow cytometry

We obtained the following anti-mouse antibodies were obtained from BD PharMingen: CD8a (53-6.7), CD4 (L3T4), CD45.1 (A20), CD44 (IM7), CD62L (MEL- 14), CD69 (H1.2F3), CD103 (M290), CD122 (TM-Beta 1). We used all antibodies at a dilution of 1/200. We purchased fluorescence-conjugated anti-mouse CD127 (A7R34) from eBioscience. To examine E- or P-selectin ligand expression, we incubated cells with rmE-Selectin/Fc Chimera or rmP-Selectin/Fc Chimera (R&D System) in conjunction with APC-conjugated F(ab9)2 fragments of goat anti-human IgG F(c) antibody (Jackson Immuno-research). We analyzed data on a FACSCanto Flow Cytometer using FACSDiva software.

Isolation of gDNA and Tcrvb (and TCRVB) high-throughput sequencing

We extracted DNA from 22-24 mg of skin (ear or de-boned tail skin), vagina, lung, gut or 6-12mg of LN using Quiagen's DNeasy mini-columns, according to the manufacturer's instruction and stored at −20°C. We then shipped it on dry ice to Adaptive Biotech. All

TCRβ characterization was performed by Adaptive Biotechnologies using the ImmunoSeq TCRβ "survey level" mouse assay. To address amplification bias in the multiplex PCR, we divided a single C57Bl/6 mouse thymus into 12 sections and TCRs ran them through HTS. Taking CDR3 sequences found in only one sample (which produces a population made up almost exclusively of CDR3 sequences represented by a single T cell in the input material), we calculated the read coverage (compared to average) associated with each V and J gene segment and used these factors to normalize sequencing output. To estimate the number of T cells bearing each rearrangement, we began with the same population of CDR3 sequences as above and calculated the mean number of sequencing reads obtained per T cell of input in this population (after normalizing for amplification bias). Next, we divided the total sequencing output of each of the 12 thymus samples by this mean coverage to estimate the number of T cells present in each of the 12 subsections. These data were used to model the relationship between the number of unique CDR3 sequences obtained and the total number of T cells sequenced. For the 12 thymus sections, these values were highly correlated (Total T cells = 1.22 * unique CDR3 rearrangements; $r^2 = 0.98$). This relationship depends on the clonal structure of the T cell population but should only depart from our model in the case of highly clonal T cell populations. In each subsequent sample this relationship was used to estimate the total number of T cells assayed and thus the mean coverage per input T cell. Finally, the number of T cells bearing each unique CDR3 sequence was estimated as (# sequencing reads obtained / estimated mean coverage). OT-I TCR tracking was based on the OT-I Vβ5.2/Dβ2/Jβ2.6 sequence TACTTCTGTGCCAGCTCTCGGGCCAAT TATGAACAGTACTTCGGTCCCGGCA- CCAGGCT (YFCASSRANYEQYFGPGTR). TCRβ characterization of human samples (n= 3 subjects) was performed using the Adaptive Biotechnologies ImmunoSeq human TCRβ assay, survey level. All raw data can be accessed at http://adaptivebiotech.com/papers/nmed69531a.

VDJ family lists corresponding to graphs in figure 2b

Mouse TCR subfamilies analyzed are described here. They are portrayed in that order in figure 2b, from left to right for both the x- and y-axis. TCR-BV1-0, -BV2-0, -BV3-0, -BV4-0, -BV5-0, -BV6-0, -BV7-0, -BV8-0, -BV9-0, -BV10-0, -BV12-1, -BV12-2, -BV12-3, -BV13-1, -BV13-2, -BV13-3, -BV14-0, -BV15-0, -BV16-0, -BV17-0, -BV19-0, - BV20-0, -BV21-0, -BV22-0, -BV23-0, -BV24-0, -BV26-0, -BV27-0, -BV28-0, -BV29-0, -BV30-0, -BV31-0. TCR-BJ1-1, -BJ1-2, -BJ1-3, -BJ1-4, -BJ1-5, -BJ1-6, -BJ1-7, -BJ2-1, -BJ2-2, -BJ2-3, -BJ2-4, -BJ2-5, -BJ2-7, -BJ1-5*1, -BJ1-5*2, -BJ1-5*3 (the last 3 using three different set of primers for the same J1-5 subtype). Human TCR subfamilies analyzed were TCR-BV01-01, BV02-01, BV04-01, -BV04-02, -BV04-03, -BV05-01, -BV05-03, -BV05-04, -BV05-05, -BV05-06, -BV05-08, -BV06-01, -BV06-04, -BV06-05, -BV06-06, -BV06-07, -BV06-08, -BV06-09, -BV07-02, -BV07-03, -BV07-04, -BV07-06, -BV07-07, -BV07-08, -BV07-09, -BV09-01, -BV10-01, -BV10-02, -BV10-03, -BV11-01, -BV11-02, -BV11-03, -BV12-01, -BV12-02, -BV12-05, -BV13-01, -BV14-01, -BV15-01, -BV16-01, -BV18-01, -BV19-01, -BV20-01, -BV21-01, -BV22-01, -BV23-01, -BV25-01, -BV27-01, -BV28-01, -BV29-01, -BV30-01 and TCR-BJ01-01, -BJ01-02, -BJ01-03, -BJ01-04, -BJ01-05, -BJ01-06, -BJ02-01, -BJ02-02, -BJ02-03, -BJ02-04, -BJ02-05, -BJ02-06, -BJ02-07. More detail is available on Adaptive's website at: http://adaptivebiotech.com/papers/nmed69531a.

Statistical analysis

We determined statistical significance in values between experimental groups using either two-way ANOVA wherever appropriate (followed by post hoc analysis using the Holm-Bonferroni method), or one-way ANOVA. The distribution and variance were normal and similar in all groups. We considered any $p>0.05$ as non-significant. In all mouse ear swelling measurement and FACS experiments, we give values as mean of independent replicates +/− standard deviation. Two way ANOVA with Holm-Bonferroni post-hoc analysis was used for **Fig. 3e, g, h, i, j**, and **l**; and **Supplementary Fig. 7d,e, f, h, j, i**, and **n**; **Supplementary Fig. 8e, f, g**, and **Supplementary Fig. 9b**. One way ANOVA was used for **Figures 3b, f, k**, and **m**; and Supplementary Fig 7g,i,k,m, o; Supplementary Fig. 8b,c,d,h; 9c,d. Each of these experiments was replicated at least once (i.e., performed twice), and typically replicated twice or more. Numbers of T cell clones cannot be assumed to follow a normal distribution, so we performed comparisons in **Supplementary Fig 6** by two-tailed Mann-Whitney U test.

Supplementary Material

Refer to Web version on PubMed Central for supplementary material.

ACKNOWLEDGMENTS

This work was supported by funding from the National Institutes of Health (R01 AR065807 to T.S.K., TR01 AI097128 to T.S.K. and R.A.C., R01 AR063962 and R01 AR056720 to R.A.C. O.G. was supported in part by the Fondation Suisse pour les Bourses en Medecine et Biologie (FSBMB).

REFERENCES

1. Bevan MJ. Memory T cells as an occupying force. Eur J Immunol. 2011; 41:1192–1195. [PubMed: 21469134]
2. Clark RA, et al. The vast majority of CLA+ T cells are resident in normal skin. J Immunol. 2006; 176:4431–4439. [PubMed: 16547281]
3. Gebhardt T, Mueller SN, Heath WR, Carbone FR. Peripheral tissue surveillance and residency by memory T cells. Trends Immunol. 2013; 34:27–32. [PubMed: 23036434]
4. Kupper TS. Old and new: recent innovations in vaccine biology and skin T cells. The Journal of investigative dermatology. 2012; 132:829–834. [PubMed: 22237702]
5. Lanzavecchia A, Sallusto F. Understanding the generation and function of memory T cell subsets. Curr Opin Immunol. 2005; 17:326–332. [PubMed: 15886125]
6. Robins HS, et al. Comprehensive assessment of T-cell receptor beta-chain diversity in alphabeta T cells. Blood. 2009; 114:4099–4107. [PubMed: 19706884]
7. Honda T, Egawa G, Grabbe S, Kabashima K. Update of immune events in the murine contact hypersensitivity model: toward the understanding of allergic contact dermatitis. J Invest Dermatol. 2013; 133:303–315. [PubMed: 22931926]
8. Jiang X, et al. Skin infection generates non-migratory memory CD8+ T(RM) cells providing global skin immunity. Nature. 2012; 483:227–231. [PubMed: 22388819]
9. Liu L, Fuhlbrigge RC, Karibian K, Tian T, Kupper TS. Dynamic programming of CD8+ T cell trafficking after live viral immunization. Immunity. 2006; 25:511–520. [PubMed: 16973385]
10. Kaech SM, Wherry EJ. Heterogeneity and cell-fate decisions in effector and memory CD8+ T cell differentiation during viral infection. Immunity. 2007; 27:393–405. [PubMed: 17892848]
11. Pepper M, Jenkins MK. Origins of CD4(+) effector and central memory T cells. Nat Immunol. 2011; 12:467–471. [PubMed: 21739668]

12. Plumlee CR, Sheridan BS, Cicek BB, Lefrancois L. Environmental cues dictate the fate of individual CD8+ T cells responding to infection. Immunity. 2013; 39:347–356. [PubMed: 23932571]
13. Tubo NJ, et al. Single naive CD4+ T cells from a diverse repertoire produce different effector cell types during infection. Cell. 2013; 153:785–796. [PubMed: 23663778]
14. Gerlach C, et al. Heterogeneous differentiation patterns of individual CD8+ T cells. Science. 2013; 340:635–639. [PubMed: 23493421]
15. Buchholz VR, et al. Disparate individual fates compose robust CD8+ T cell immunity. Science. 2013; 340:630–635. [PubMed: 23493420]
16. Campbell JJ, O'Connell DJ, Wurbel MA. Cutting Edge: Chemokine receptor CCR4 is necessary for antigen-driven cutaneous accumulation of CD4 T cells under physiological conditions. J Immunol. 2007; 178:3358–3362. [PubMed: 17339428]
17. Robins H, et al. Ultra-sensitive detection of rare T cell clones. J Immunol Methods. 2012; 375:14–19. [PubMed: 21945395]
18. Sherwood AM, et al. Deep sequencing of the human TCRgamma and TCRbeta repertoires suggests that TCRbeta rearranges after alphabeta and gammadelta T cell commitment. Sci Transl Med. 2011; 3:90ra61.
19. Popov A, Mirkov I, Kataranovski M. Inflammatory and immune mechanisms in contact hypersensitivity (CHS) in rats. Immunol Res. 2012; 52:127–132. [PubMed: 22388639]
20. Christensen AD, Haase C. Immunological mechanisms of contact hypersensitivity in mice. APMIS. 2012; 120:1–27. [PubMed: 22151305]
21. Liu L, et al. Epidermal injury and infection during poxvirus immunization is crucial for the generation of highly protective T cell-mediated immunity. Nat Med. 2010; 16:224–227. [PubMed: 20081864]
22. Gulati N, et al. Molecular characterization of human skin response to diphencyprone at peak and resolution phases: therapeutic insights. J Invest Dermatol. 2014; 134:2531–2540. [PubMed: 24751728]
23. Watanabe R, et al. Human skin is protected by four functionally and phenotypically discrete populations of resident and recirculating memory T cells. Science translational medicine. 2015; 7:279ra239.
24. Moon JJ, et al. Quantitative impact of thymic selection on Foxp3+ and Foxp3- subsets of self-peptide/MHC class II-specific CD4+ T cells. Proceedings of the National Academy of Sciences of the United States of America. 2011; 108:14602–14607. [PubMed: 21873213]
25. Mackay LK, et al. The developmental pathway for CD103(+)CD8+ tissue-resident memory T cells of skin. Nat Immunol. 2013; 14:1294–1301. [PubMed: 24162776]

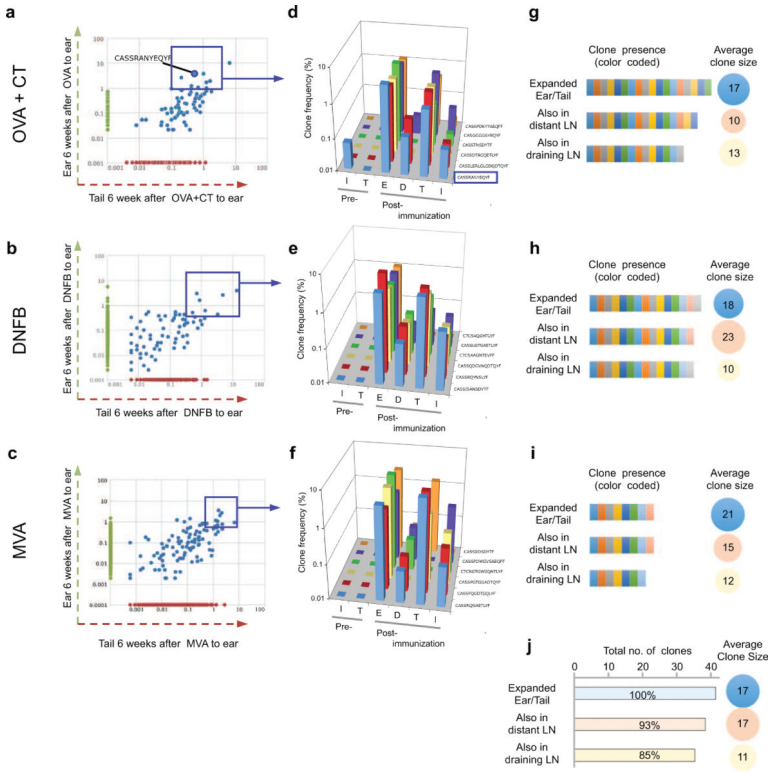

Figure 1. Skin immunization generates skin T_{RM} and TCR-identical T_{CM} in LN

(**a**), (**b**) and (**c**) Dot plots of the frequency (number of a given sequence divided by the total number of sequences observed in the given sample) of TCRβ CDR3 sequences shared in antigen-exposed (ear, green vertical axis) and distant (tail, red horizontal axis) skin after OVA+CT immunization (**a**), DNFB sensitization (**b**), and MVA skin scarification (**c**). Each blue dot represents a T cell clone with a unique CDR3 sequence, and the most abundant expanded clones are enclosed in the blue rectangle. In (**a**), the OT-I Vβ CDR3 sequence (CASSRANYEQYF) is highlighted (n=3 mice per antigen). (**d**), (**e**), (**f**), Tracking of selected abundant TCRβ CDR3 sequences (**d**[OVA+CT], **e**[DNFB], **f**[MVA]) identified in (**a**), (**b**) and (**c**), respectively. I: inguinal LN; T: tail skin; E: Ear skin; Draining LN (ear-draining); T: tail skin; I: inguinal LN. Data for CDR3 sequences (TCR percentage) are shown as the percentage (specific/total) of CDR3 sequences (n=3 mice per antigen) from T cell clones present at n≥5 copies in skin assessed in other tissues. (**g**), (**h**), (**i**) Unique expanded clones (**g**[OVA+CT], **h**[DNFB], **i**[MVA])are indicated by colored contiguous rectangles, and the corresponding clones (each color is a unique clone) present in draining, and distant LN are shown in the same fashion. The average clone size in each compartment is shown to the right in the colored circle. (**j**) total number of T cell clones (n≥5 per clone, horizontal bar graphs) and mean clone size (colored circle) in the tissues of all mice combined (immunized with OVA+CT, DNFB, or MVA). (n=9 mice).

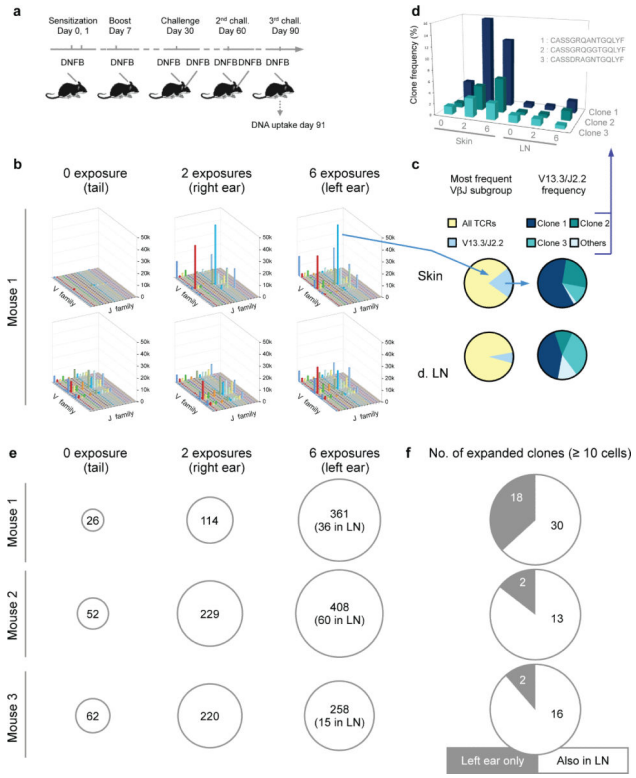

Figure 2. Repetitive sensitization increases the abundance of T_{RM} in skin

(**a**) Temporal scheme of the repetitive DNFB sensitizations and challenges. (n=3 mice for each condition, all experiments performed 2-3 times, representative data is shown). (**b**) Frequency of respective beta chain V and J α T cell populations in the skin and LN of the repetitively immunized mice at day 91. The x-axis shows the TCR Vβ subtype (described in detail in methods), the y-axis their frequency, and the z-axis shows the TCR Jβ subtype. The VβJβ repertoire observed in different skin areas (upper) exposed to DFNB as well as the respective draining LN (lower graphs; inguinal, right and left submandibular LN respectively). (n=3 mice). (**c**) The left pie chart represents the frequency of the highly expanded V13.3/J2.2 clones in the left ear of DNFB sensitized, boosted and challenged mice, both in the left ear and left cervical (draining) LN. The right pie chart represents the three most abundant individual TCR clones (unique CDR3 sequences) comprising this specific VJ subgroup, plus all other minor clones from this VJ subgroup in pale blue. (n=3 mice). (**d**) Clone frequency of the three most abundant TCR CDR3 sequences (depicted in **c**) skin and tail after 0,2, and 6 DNFB exposures. (**e**) The single most abundant T cell clone in skin exposed 0×, 2×, and 6× to DNFB in each of three mice, expressed as T cells/400ng gDNA . The copy number of the same clone in LN is shown in parentheses (in the 6× circle), n=3 mice. (**f**) Number of highly expanded clones present in at least 10 copies per 400ng of tissue in the skin and LN of the immunized mice, showing skin-specific (T_{RM}) increase (n=3 mice).

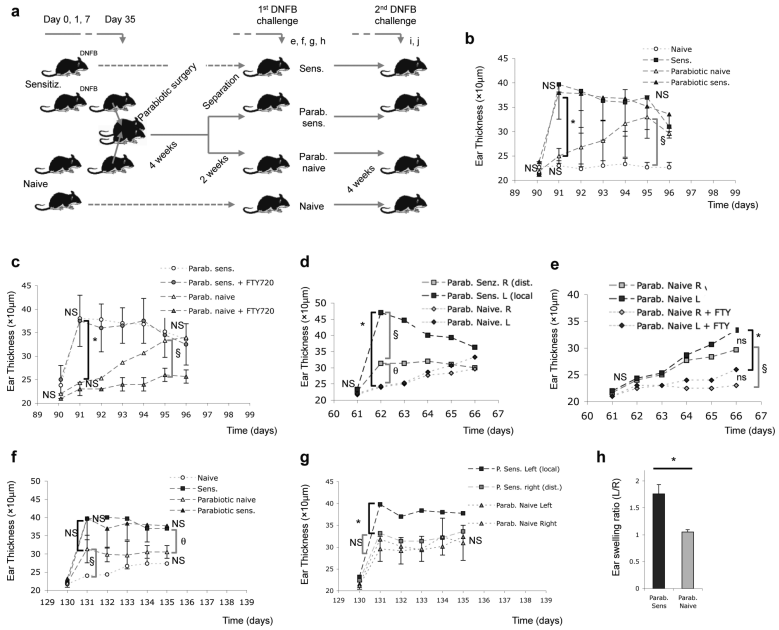

Figure 3. T_{RM} mediate rapid CHS responses, while T_{CM} mediate delayed attenuated CHS responses

(**a**) Experimental plan for the subsequent experiments (n=3 pairs of parabiotic mice; n=3 for naive and sensitized non-parabiotic controls, respectively). Experiments were performed 2-4 times. (**b**) Ear swelling kinetics in parabiotic sensitized and parabiotic naive mice, with non-parabiotic sensitized and naive mice as controls. (*p=0.001; § p=0,005, n=3 in each group). (**c**) An identical experiment to that shown in (**b**) was performed, but this time mice were pre-treated with FTY-720 (*p=0.002; § p=0.002, n=3 per group). (**d**) Comparison of the ear swelling kinetics after DNFB challenge at the initial (local) site of immunization (Left) and at a distant site (Right) in parabiotic sensitized mice. In parabiotic naive mice, the Left and Right ears were measured after DNFB challenge (these parabiotic naive mice had not been sensitized) (*p=0.001; § p=0.01; $^{\theta}$p=0.02, n=5 mice in each group). (**e**) Kinetics of left and right ear swelling after DNFB challenge in parabiotic naive mice, with or without FTY-720 treatment. (*p=0.001; § p=0.001, n=5 mice in each group). (**f**) Left ear swelling after the final (2nd) DNFB challenge in parabiotic naive and parabiotic sensitized mice, treated as shown in (**a**), with non-parabiotic naive and sensitized mice as controls (see panel d) (§ p=0.04; $^{\theta}$p=0.001, n=5 mice in each group). (**g**) Left (local) vs. right (distant) ear swelling after the final DNFB challenge parabiotic naive and parabiotic sensitized mice (*p=0.04, n=3 in each group). (**h**) Ratio (%) of the left vs right maximal ear swelling after the second challenge in the sensitized vs. naïve parabiotic mice. (p=0.029, n=3 in each group). All results show mean +/− SD. Statistical analysis using two way ANOVA with Holm-Bonferroni post hoc analysis where appropriate, or one way ANOVA only, were used (see Materials and Methods). P>0.05 was considered not significant (ns).

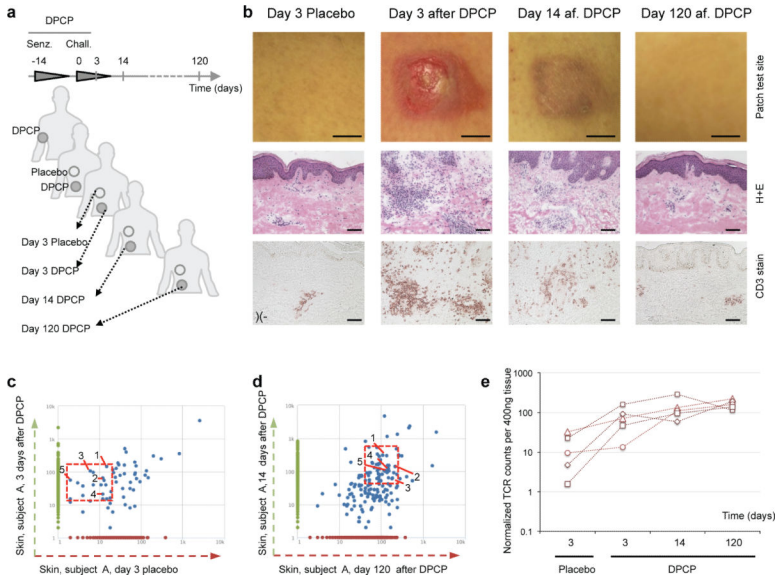

Figure 4. Contact dermatitis to DPCP induces T_{RM} cells in human skin

(**a**) Schematic of DPCP sensitization and sample recovery. (**b**) Clinical photos, hematoxylin-eosin histology and $CD3^+$ T cell staining at day 3 (placebo and DPCP challenged), 14 (DPCP challenged) and 120 (DPCP challenged) of the skin of subjects, at indicated time points. (Representative data are shown from a total of 11 subjects entered in the study). (**c**) Dot plots of the frequency (number of a given sequence divided by the total number of sequences observed in the given sample) of TCRβ CDR3 sequences shared (or not) in non-exposed or DPCP-exposed skin from a representative individual. The left panel shows clones in 4 day post DPCP challenge site skin (vertical axis) vs. the same time point in placebo challenged skin (horizontal axis). Clones present in both sites are shown as blue dots. Five clones are identified (1-5) for subsequent reference. The right panel shows clones 14 days post DPCP challenge (vertical axis) vs clones 4 months after DPCP challenge. The same five clones are identified as being present in both samples. (**d**) quantification of the T cell clone size observed in **c** over time. (n=3 out of 11 subjects: F, 48; M, 52; M, 55; biopsies were subjected to HTS; data from one representative patient shown).